REPORT DOCUMENTATION PAGE

Form Approved OMB NO. 0704-0188

1. REPORT DATE (DD-MM-YYYY)	2. REPORT TYPE	3. DATES COVERED (From - To)
	New Reprint	-

4. TITLE AND SUBTITLE
Triangular Graphene Grain Growth on Cube-Textured Cu Substrates

5a. CONTRACT NUMBER
W911NF-09-1-0295

5b. GRANT NUMBER

5c. PROGRAM ELEMENT NUMBER
611102

6. AUTHORS
Jianwei Liu, Judy Wu, Christina M. Edwards, Cindy L. Berrie, David Moore, Zhijun Chen, Victor A. Maroni, M. Parans Paranthaman, Amit Goyal

5d. PROJECT NUMBER

5e. TASK NUMBER

5f. WORK UNIT NUMBER

7. PERFORMING ORGANIZATION NAMES AND ADDRESSES
University of Kansas Center for Research, Inc.
2385 Irving Hill Road
Lawrence, KS 66045 -7568

8. PERFORMING ORGANIZATION REPORT NUMBER

9. SPONSORING/MONITORING AGENCY NAME(S) AND ADDRESS(ES)
U.S. Army Research Office
P.O. Box 12211
Research Triangle Park, NC 27709-2211

10. SPONSOR/MONITOR'S ACRONYM(S)
ARO

11. SPONSOR/MONITOR'S REPORT NUMBER(S)
56050-EL.10

12. DISTRIBUTION AVAILIBILITY STATEMENT
Approved for public release; distribution is unlimited.

13. SUPPLEMENTARY NOTES
The views, opinions and/or findings contained in this report are those of the author(s) and should not contrued as an official Department of the Army position, policy or decision, unless so designated by other documentation.

14. ABSTRACT
The growth of graphene has been carried out on cube-textured (100) oriented Cu (CTO-Cu) foils using chemical vapor deposition (CVD). Well-aligned triangular grains self-assembled on CTO-Cu during CVD heating in fl owing hydrogen. The nucleation of triangular graphene grains has been confi rmed. This demonstrates that the shape and possible alignment of the graphene

15. SUBJECT TERMS
graphene, controlled growth, copper, cubic texture

16. SECURITY CLASSIFICATION OF:			17. LIMITATION OF ABSTRACT	15. NUMBER OF PAGES	19a. NAME OF RESPONSIBLE PERSON
a. REPORT	b. ABSTRACT	c. THIS PAGE			Judy Wu
UU	UU	UU	UU		19b. TELEPHONE NUMBER: 785-864-3240

Report Title

Triangular Graphene Grain Growth on Cube-Textured Cu Substrates

ABSTRACT

The growth of graphene has been carried out on cube-textured (100) oriented Cu (CTO-Cu) foils using chemical vapor deposition (CVD). Well-aligned triangular grains self-assembled on CTO-Cu during CVD heating in fl owing hydrogen. The nucleation of triangular graphene grains has been confi rmed. This demonstrates that the shape and possible alignment of the graphene grains can potentially be tuned by changing the properties of the substrate, which should ultimately lead to improved electrical properties of the graphene. This type of graphene nucleation and alignment is novel and has not been observed in previous studies on other copper foil samples.

REPORT DOCUMENTATION PAGE (SF298)
(Continuation Sheet)

Continuation for Block 13

ARO Report Number 56050.10-EL
Triangular Graphene Grain Growth on Cube-Tex ...

Block 13: Supplementary Note

Approved for public release; distribution is unlimited.

FULL PAPER

Triangular Graphene Grain Growth on Cube-Textured Cu Substrates

Jianwei Liu, Judy Wu, Christina M. Edwards, Cindy L. Berrie, David Moore, Zhijun Chen, Victor A. Maroni, M. Parans Paranthaman, and Amit Goyal*

The growth of graphene has been carried out on cube-textured (100) oriented Cu (CTO-Cu) foils using chemical vapor deposition (CVD). Well-aligned triangular grains self-assembled on CTO-Cu during CVD heating in flowing hydrogen. The nucleation of triangular graphene grains has been confirmed. This demonstrates that the shape and possible alignment of the graphene grains can potentially be tuned by changing the properties of the substrate, which should ultimately lead to improved electrical properties of the graphene. This type of graphene nucleation and alignment is novel and has not been observed in previous studies on other copper foil samples.

1. Introduction

Graphene has attracted much attention recently due to its remarkable mechanical, electrical and optical properties.[1,2] Graphene is a gapless semiconductor with extremely high carrier mobility and a single layer of graphene absorbs only 2.3% of visible light.[3,4] Many applications have been projected for graphene and exciting progress has been made as demonstrated in several technologies including transistors,[5] alternative transparent conductors to Indium-Tin-Oxide,[6,7,8] photovoltaic devices,[9,10] sensors,[11,12,13] and energy storage devices.[14] A primary challenge in the application of graphene is in epitaxy of large-area graphene with controlled thickness and low defect density.[5,15,16] Chemical vapor deposition (CVD) of graphene on metal foils such as Cu is particular attractive since the graphene thickness is typically restricted to 1-2 layers due to low solubility of C in Cu. Large area growth has been demonstrated recently.[17,18,19] Unfortunately, the carrier mobility in CVD graphene on polycrystalline Cu foils (Poly-Cu) is significantly lower than that observed on exfoliated graphene, most likely due to the presence of a large number of grain boundaries (GBs) and other growth defects.[18,19,20,21] Considering the small grain size in CVD graphene (on the order of microns) in contrast to the size of graphene sheets needed in practical applications with dimensions up to meters, the effect of GBs on the charge transport will be important. Controlling GBs so as to minimize the charge scattering effect by GBs is essential in order to bring the charge mobility up to its intrinsic limit in graphene.

Poly-Cu foils are commercially available at low cost with large areas and have been used widely as substrates for CVD graphene. On Poly-Cu, multiple graphene grains of different in-plane orientations initiate simultaneously from the same nucleation site.[20,21,22] This may be attributed to multiple Cu (111) facets with different crystallographic orientations existing in proximity on the Poly-Cu surface and large-angle GB's are hence unavoidable features on graphene grown on Poly-Cu.[20,21,23] Single crystal Cu (SC-Cu) (111) surfaces are ideal for graphene epitaxy but SC-Cu foil is expensive and not available in larger size. In this work, we report the growth of graphene on cube-textured (100) oriented Cu (CTO-Cu) foils using chemical vapor deposition (CVD). The nucleation of triangular graphene grains has been confirmed. It should be mentioned that rectangle (triangle) graphene flakes were obtained on the rectangle pits formed during thermal annealing on Co (or Ni) films deposited on MgO (100) substrates (or triangular pits if on MgO (111) substrates).[24] Since no graphene could grow on the flat Co (or Ni) areas, a mechanism of simultaneous formation of pits and nucleation of graphene was proposed.[24] Note the pit dimension is fixed during graphene growth. Therefore, no continuous sheets of graphene can be obtained using the approach. This is in contrast to the evolution of the triangular graphene grains into a continuous graphene sheet as the grains grow and coalesce, which is not surprising considering the difference in graphene nucleation on Cu as compared to on Co and Ni. Moreover, the in-plane texture of the CTO-Cu provides an alignment mechanism for the triangles in addition to the shaping effect, resulting in predominantly aligned right triangle arrays on CTO-Cu foils. These single crystal cubic, (111)

Dr. J. Liu, Prof. J. Wu
Department of Physics and Astronomy
University of Kansas
Lawrence, KS, USA 66045
E-mail: liuw@ku.edu
C. M. Edwards, Prof. C. L. Berrie, Dr. D. Moore
Department of Chemistry, University of Kansas
Lawrence, KS, USA 66045
Dr. Z. Chen, Dr. V. A. Maroni
Materials Science Division
Bldg 212, Argonne National Laboratory, Argonne, IL, USA 60439
Dr. M. P. Paranthaman
Chemical Sciences Division
Oak Ridge National Laboratory, Oak Ridge, TN, USA 37831
Dr. A. Goyal
Materials Science & Technology Division
Oak Ridge National Laboratory, Oak Ridge, TN, USA 37831

DOI: 10.1002/adfm.201101305

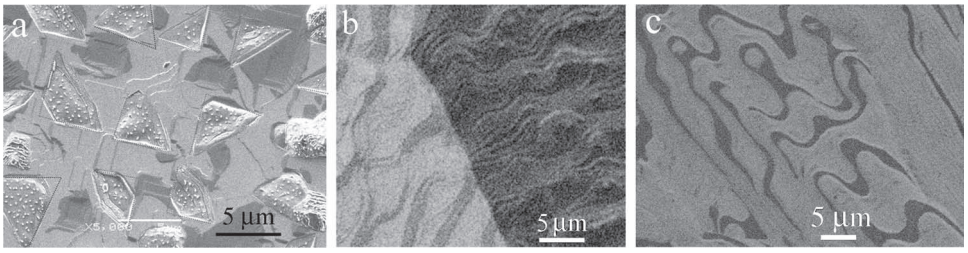

Figure 1. a) SEM image of CTO-Cu heated to 1000 °C under 2 sccm H_2 flow followed by cooling to room temperature. b) SEM image of CTO-Cu annealed at 1000 °C for 20 min under 2 sccm H_2 flow before cooled to room temperature, c) SEM image of Poly-Cu heated to 1000 °C under 2 sccm H_2 flow followed by cooling to room temperature.

oriented traingles with several micrometers in dimension provide ideal nucleation sites for graphene epitaxy and the details of the expriment is described in the following.

2. Results and Discussion

2.1. The Effect of Annealing on the Morphologies of Cu Foils

Following the procedure in the Experimental Section, graphene films have been grown using CVD on CTO-Cu substrates. The effect of annealing of the CTO-Cu was investigated by heating the substrate under a hydrogen flux for different lengths of time. The same heating procedure was applied to CTO-Cu and Poly-Cu foils for comparison. A heating rate of 20 °C/min was adopted to heat the samples to 1000 °C in H_2 flow followed by immediate cooling back to room temperature (cooling took about 2 hours) by turning off the furnace. **Figure 1** compares the CTO-Cu and Poly-Cu surface morphology after the substrate had been heated to 1000 °C in H_2 flow followed by cooling back to room temperature immediately without annealing process [Figure 1a] and after a 20 minute annealing at 1000 °C [Figure 1b]. Triangles of a few μm in dimension can be clearly seen in the former while only surface steps are shown in the latter. The fact that the triangles are eliminated through additional annealing in H_2 suggests the triangles are most probably surface features of copper oxides due to residual oxygen in CTO-Cu and in the CVD chamber. This argument is supported by the visibility of the grain boundaries of the CTO-Cu (the line separating two domain areas of different brightness) in the annealed CTO-Cu in Figure 1b and the electron backscattering diffraction (EBSD) pattern (not shown) that can be indexed to Cu (100) as expected. Such a pattern cannot be detected on the samples without H_2 annealing, suggesting the surface is covered with a thick (possibly several to tens of nm) amorphous layer of Cu-O either on or away from the triangles. The triangle features appeared on CTO-Cu over the entire range of conditions explored in this experiment (H_2 flow rate: 0.1 – 2 sccm, H_2 partial pressure 30-120 mTorr). In addition, the triangle features are unique to CTO-Cu since they did not appear on the Poly-Cu foils processed in the same runs without annealing process (Figure 1c). It should be noted that the majority of the triangles are right triangles with the two shorter sides (red dashed lines are shown in Figure 1a for guidance of eyes) aligned with respect to each other within 5 degree. Considering the four-fold symmetry of the (100) CTO-Cu, the shape and alignment of the triangles might be attributed to the influence of the in-plane texture of the CTO-Cu.

2.2. The Growth and Characterization of Triangular Graphene Grains on CTO-Cu

The growth of graphene initiated on the triangles after CH_4 was introduced into the CVD chamber immediately after the growth temperature of 1000 °C was reached. **Figure 2** shows the SEM images of graphene nuclei on CTO-Cu after 5 minutes of CVD growth. The graphene nuclei on CTO-Cu [Figure 2a and 2b] have distinctive triangle shapes of lateral dimension on the order of several micrometers. Many triangles on the CTO-Cu are predominantly in the shape of right triangles with one shorter side aligned approximately along the direction shown in the dashed lines in Figure 2a. In some cases, equilateral triangles are also observed [see for example blue highlighted triangles in Figure 2a and 1a]. AFM images of these samples are consistent with the SEM images and allow the shape of the triangle to be investigated in more detail. The representative AFM images taken on and away from the triangless and cross-sectional cuts through the images are shown in Figure 2c–2d. These triangle features are typically on the order of 80–150 nm tall from edge to center and show clear faceting along different directions [Figure 2c]. The regions outside the triangular area show very rough topography, again consistent with the SEM images. The roughness in these regions is on the order of 10–15 nm [Figure 2d], which is much larger than the expected thickness of an adsorbed hydrocarbon layer. A surface coating of this thickness (most probably amorphous copper oxide) would mask the ability to observe the crystalline nature of the copper substrate beneath the layer. This argument is supported by the uniform distribution of chemical elements C, O and Cu as shown in the line scans across a selected triangle in Figure 2e using energy-dispersive X-ray spectrometry (EDS). The presence of oxygen may be attributed to absorbed gaseous molecules from residual air on Cu surface, which may be difficult to avoid considering CVD is a low vacuum process. This residual oxygen may form copper oxide on the surface as well, which could inhibit the nucleation of the graphene, except where that oxide is reduced, such as on the triangles. Considering the oxygen content has negligible variation across the triangles, the reduction may occur only on the surface of the triangles. A more detailed discussion will be given later.

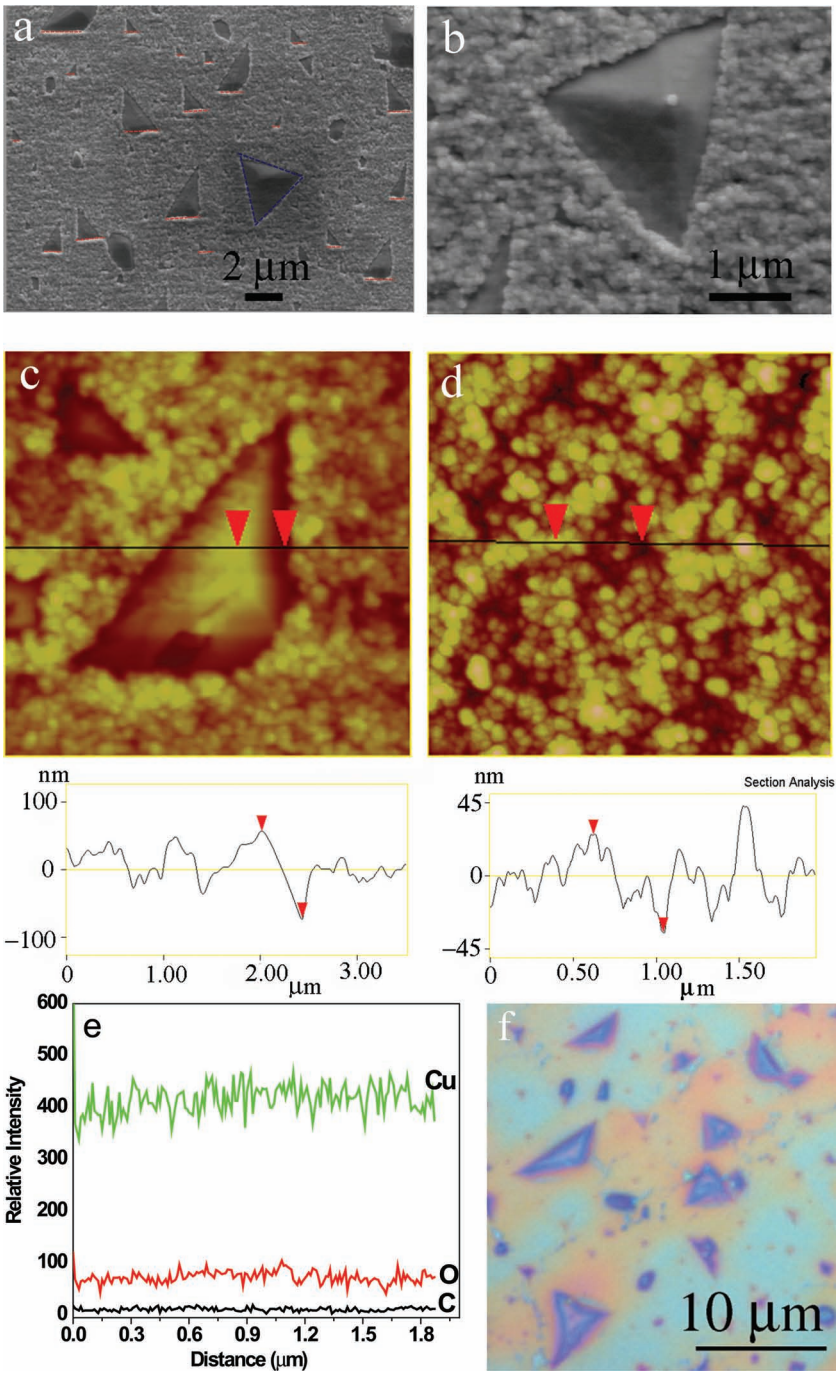

Figure 2. SEM and AFM images of graphene grown on CTO-Cu using CVD method for 5 min. a) SEM image of graphene grown on CTO-Cu. b) High-resolution SEM image of a triangle. c) AFM image of a triangle of graphene & section analysis. d) AFM image of background region & section analysis. e) EDS line scan of Cu, O and C across the line in the triangle shown in the inset. f) Optical image of transferred graphene grown on CTO-Cu.

In order to confirm graphene nucleation on the triangles, graphene was transferred onto Si substrates with a thermal SiO_2 layer of 300 nm in thickness for clear visibility of the single-layer graphene.[1] The optical image of transferred graphene grown on CTO-Cu for 5 minutes is shown in Figure 2f. The triangular graphene domains with dimensions up to several μm are consistent with those observed in the SEM images before transfer, shown in Figure 2a. This suggests that the graphene nucleate only on these triangular regions of the surface, which appear through the EBSD data taken on the triangles [see **Figure 3**a], to be predominantly Cu (111) oriented regions.

No EBSD patterns can be detected on areas away from triangles [Figure 3b] while clear EBSD patterns are observed on all triangles as shown in Figure 3d–3f. The EBSD patterns obtained from the triangles can be indexed predominatly to the Cu (111) out-of-plane within serveral degrees with respect to the standard pole using TSL OIM Analysis 5 software as shown in Figure 3c, which may be due to the pyramidal shape of the triangles confirmed in the AFM image in Figure 2c. Because the lattice of Cu (111) (2.56 Å) matches well with the lattice of graphene (2.46 Å),[25] it is difficult to distinguish the EBSD patterns from Cu (111) and graphene directly although Cu (111) facet provides an ideal surface for graphene epitaxy. Since the graphene films are only 1 layer thick based on the optical transmittance measurement, it is therefore likely that the patterns observed are mostly due to the structure of the Cu underneath the graphene since the penetration depth of the electron beam is far beyond 1 layer. Some subtle differences in the morphology of the graphene triangles have been observed. While most triangles in Figure 2 and 3 have a pyramidal shape with three distinctive edges extending from the top to the vertices, some triangles with flat tops have also been observed [the inset of Figure 3a]. The pyramidal nature of the features observed in the AFM images again suggests that the underlying structure is a result of the triangle structure underneath the graphene. Otherwise, such large topographic variations would not be observed for single layer graphene. Furthermore, the optical transmittance of graphene grown on CTO-Cu for 30 min is 97% at 550 nm wavelength, which is close to the expected best transmittance of graphene (97.7%).[4] It is of particular importance that the same EBSD pattern was observed on different locations of the same triangle, as shown in Figure 3d–3f, indicating the Cu triangles formed on the CTO-Cu substrate are single crystalline. This presents the possibility for the triangle graphene grains grown on individual (111) oriented triangles on CTO Cu to be single crystalline as suggested by recent work of graphene epitaxy on Cu (111) single crystal substrates.[25] This differs from the results reported previously on Poly-Cu foils on which the graphene nuclei are polycrystalline with multiple branches (such as a four-lobed shape) of different in-plane orientations initiating

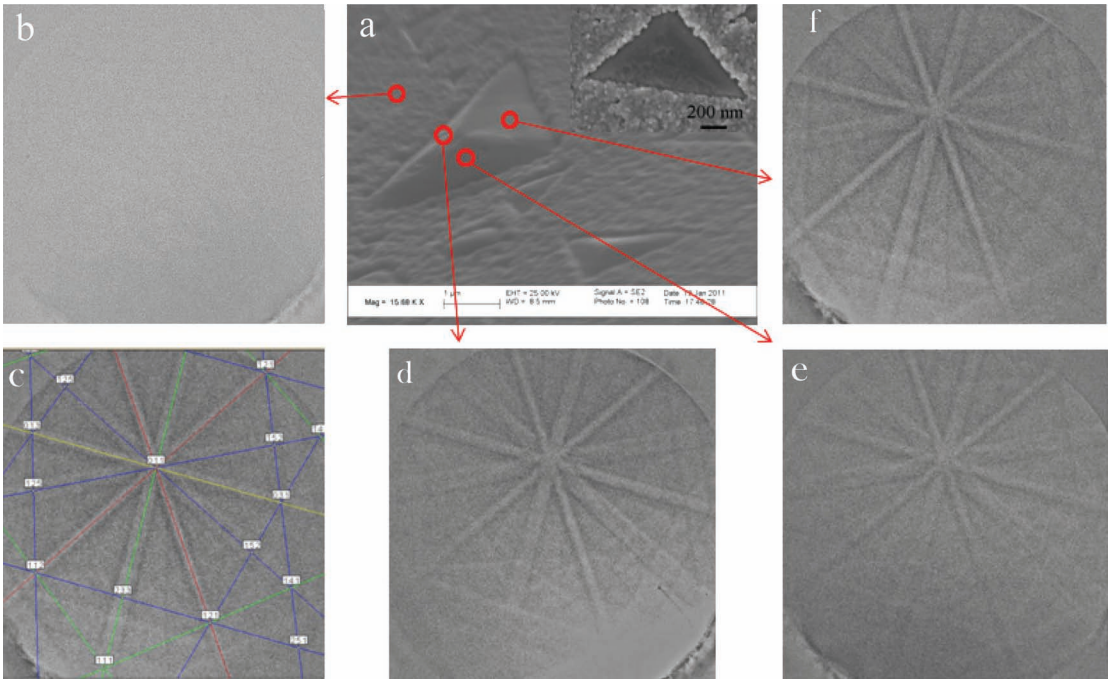

Figure 3. SEM image and EBSD patterns of triangular graphenes. a) SEM image of graphene triangles on CVD CTO Cu. (inset showed SEM image of triangle with a flat top). b) EBSD pattern taken away from triangles. (d-f) EBSD patterns on different facets of the triangle on CTO-Cu. c) EBSD pattern indexed to Cu(111).

from the same nucleation sites.[20] It should be realized that Cu (111) should have three-fold symmetry and hence mainly equilateral triangles were expected. The observation of predominantly (111) oriented, right triangles on CTO-Cu foil suggests an important role the substrate plays on the shape as well as alignement of the triangles. Understanding the in-plane crystallographic orientation of the triangles with respect to the CTO-Cu substrate is a focus of our ongoing research and could lead to schemes for controlling the graphene grain alignment in large scale.

2.3. The Evolution of Triangular Graphene Grains on CTO-Cu

With an increase of the growth time, the graphene triangles on CTO-Cu extend to larger size and merge together between two neighboring grains. **Figure 4**a and b include the SEM images of graphene on CTO-Cu with growth time of 10 and 30 minutes, respectively. On the former some merged triangle graphene grains are visible while on the latter, multiple terraces form as consequence of Cu surface evolution.[26] In fact, some short terraces appeared already at the 10 minute growth time [arrows in Figure 4a]. A comparative study of Cu surface morphology (data not shown) after annealing at 1000 °C showed the change in the morphology of the copper is much larger when Cu foils were exposed to the gas mixture required for graphene growth than it is when simply annealed in vacuum.

After 12–15 minutes of growth, a full coverage of graphene on CTO-Cu was observed. Since the graphene growth stops after the Cu surface is covered completely, longer time growth up to 30 minutes was made to obtain a continuous sheet of graphene. Representative Raman spectra taken on graphene grown on CTO-Cu and Poly-Cu grown simultaneously for 30 min are shown in **Figure 5**. Two intense features are observed: the G peak at around 1580 cm^{-1} due to the doubly degenerate zone center E_{2g} mode and the 2D peak at around 2700 cm^{-1} arising from the second order zone-boundary phonons.[27] The full-width-at-half-maximum (FWHM) is around 50 cm^{-1}. This demonstrates the absence of interlayer coupling at the excitation wavelength of 442 nm, since such coupling would result in an increase in the FWHM to approximately 100 cm^{-1}. The ratio of the intensities of the single sharp

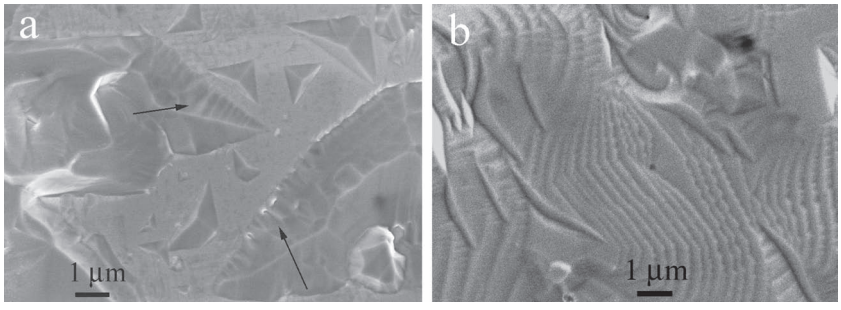

Figure 4. SEM images of CVD graphene on CTO-Cu. a) SEM image of graphene on CTO-Cu with a growth time of 10 min. b) Growth time of 30 min. Arrows in (a) indicate appearance of terraces on merged graphene grains.

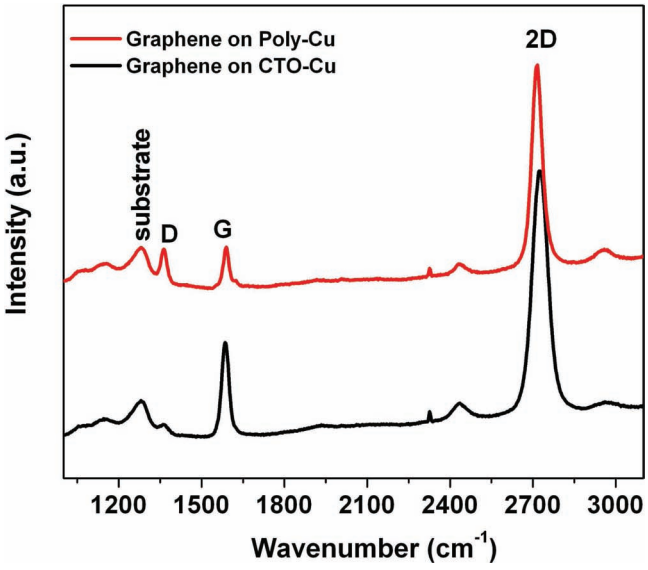

Figure 5. Raman spectra of graphene grown on CTO-Cu for 30 min (solid black line) and graphene on Poly-Cu (solid red line) under the same growth conditions.

2D peak to the G peak are observed to be greater than a factor of two and also show typical symmetric features, indicating the presence of single layer graphene.[19] Furthermore, for the Raman spectrum taken from the graphene grown on CTO-Cu, the D peak at ~1350 cm^{-1} due to the breathing modes of sp^2 rings and the active phonons being excited in defective regions of the graphene is very small, indicating the absence of a significant number of defects on the graphene grown on CTO-Cu. The intensity of the D peak to that of the G peak (I_D/I_G) may be used to estimate the defect density in graphene.[28] The ratio of I_D/I_G of graphene grown on CTO-Cu is around 0.2, which is considerably smaller than that of graphene on Poly-Cu (0.56), indicating a much lower density of defects on graphene grown on CTO-Cu as compared to that on Poly-Cu. A possible explanation is the reduction of GBs and related growth defects graphene nucleated on single crystal Cu (111) triangles formed on CTO-Cu.

2.4. The Formation Mechanism of Triangular Graphene Grains on CTO-Cu

To obtain an understanding of the mechanism underlying triangle formation, some quenched graphene on CTO-Cu samples were treated with 0.1 M HCl solution briefly (~2 sec) to remove the surface oxide layer together with graphene nuclei. **Figure 6** shows the SEM images of a graphene sample on CTO-Cu with 5 min growth time (a similar sample to that shown in Figure 2) after the HCl treatment. It is noticeable that the bases of many triangles remained (Figure 6a and 6b) and they consist of a large number of nanoparticles with irregular shapes. Many of the nanoparticles seem to have sharp edges and vertices, suggesting they may have crystalline structures. On the very top surface of the triangles, a layer of predominantly equilateral triangles can be seen [Figure 6c and 6d], which suggest they may be the (111) crystallites responsible for the EBSD patterns in Figure 3. It is well known that metal oxides may epitaxially form on (100) oriented metals, such as Ni[29] and Cu.[30,31] In particular, (111) Cu_2O of thickness in several tens of nm may nucleate in the from of nanoparticles on (100) orientated Cu at elevated temperature due to the presence of the sub-surface oxygen.[30,31] If migration of these (111) Cu_2O nanoparticles becomes possible, larger dimension grains will form as a consequence of the migration. Based on this information, we hypothesize a model as shown schematically in Figure 6e. At the moderate H_2 partial pressure used in this experiment, the reduction of the Cu_2O surface layer during CVD heating may not be adequate. Previous investigation demonstrated that the reduction rate of CuOx decreases with decreasing H_2 partial pressure.[32] According to the Cu-O phase diagram,[33] the eutectic temperature of Cu-CuO and Cu-Cu_2O are 1091 °C, and 1066 °C, respectively, which are close to the growth temperature of graphene at 1000 °C in this work. On the other hand, the solubility of hydrogen in Cu increases with temperature,[34] resulting in Cu-O-H intermediate phases on the substrate surface at elevated temperatures. Premelting[35] (partial melting) within a thin layer close to the surface of the Cu may occur at temperatures considerably lower than the bulk melting point of Cu (1083 °C) depending on the crystallographic orientation at the surface and existence of impurities,[36] such as CuOx and H_2. During the premelting process, the mobility of CuOx may be considerably enhanced, resulting in formation of Cu_2O crystallites (or nanoparticles) that are highly mobile due to the surface layer of Cu-O-H. The domains with shape-complementarity tend to aggregate into triangles. Self-assembly of the Cu_2O crystallites into aligned triangles may be facilitated by the surface orientation on CTO-Cu. Since (111) is the energetically preferred orientation of cubic Cu_2O, the nanoparticles may assemble into triangles with Cu_2O (111) orientation. The in-plane (100) texture of the CTO-Cu may provide shape restriction and alignment to the crystallite self-assembly, resulting in right triangles with their shorter sides aligning in the (100) or (010) directions of the CTO-Cu substrate, instead of equilateral triangles.[37] The graphene can nucleate on the triangles as soon as the reduction occurs on the surface of the triangles to expose the Cu (111), which provides the lattice match to graphene. Reduction on other areas away from the triangles seems to occur more slowly due to possibly much thicker Cu-O-H layer. This result in graphene growth initiated from the triangles dominating the entire graphene nucleation.

3. Conclusions

In summary, CTO-Cu foil presents a novel potential substrate for the epitaxy of graphene through provision of well-aligned single crystalline grains self-assembled on the substrate surface during CVD heating in H_2 flux. The (111) oriented, triangular facets exposed through reduction at the surface of the triangles provide ideal nucleation sites for growth of graphene grain. The in-plane crystallographic texture of the CTO-Cu substrate was found to play an important role in defining the shape and alignment of the triangles. Crystallographic alignment is critical for optical properties of the graphene, and the reduction of the amount of large-angle grain boundaries may explain the lower defect intensity in the Raman spectra taken on graphene/CTO-Cu as compared to graphene/poly-Cu grown at the same conditions.

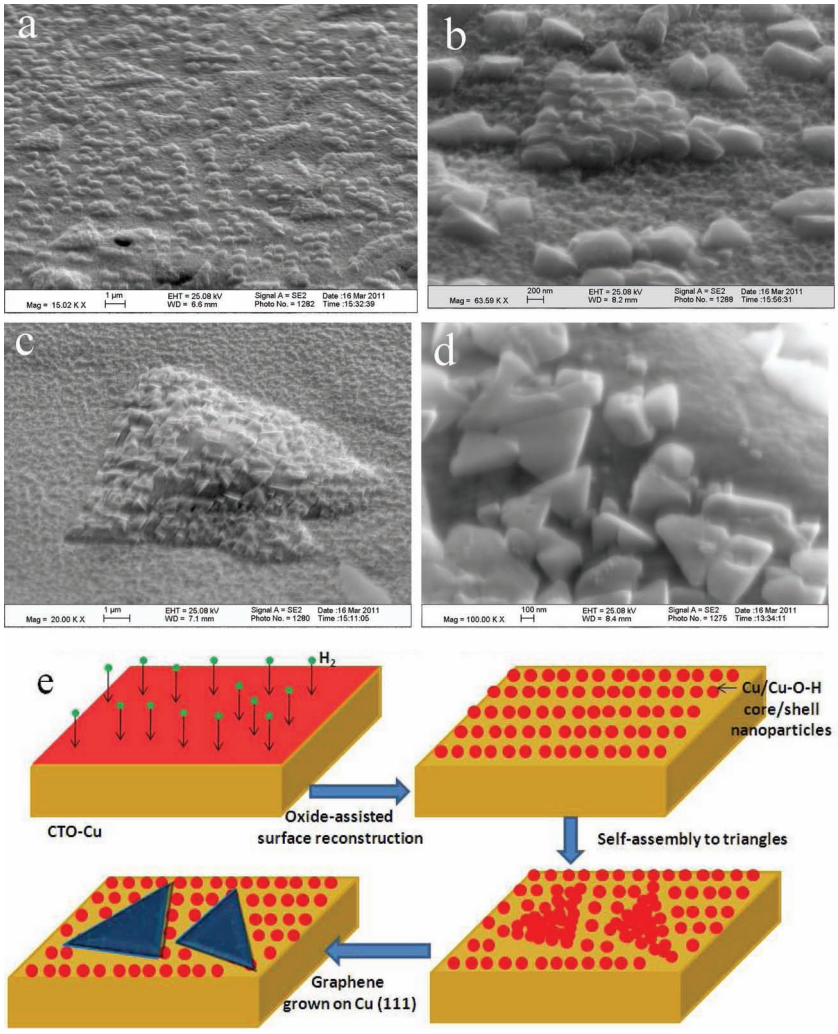

Figure 6. SEM images and schematic description of the formation of triangular graphenes on CTO-Cu. a) and b) SEM images of graphene grown on CTO-Cu for 5 min etched in the 0.1 M HCl solution for 2 seconds at different scales. c) A typical triangle grain covered with small nanoparticles. d) A zoomed in view of the nanoparticles revealing equilateral triangle-shaped nanoparticles. e) Schematic description of the surface self-assembly process occurred on CTO-Cu during CVD heating in H_2 flow: formation of a surface Cu-O-H layer (red color) upon diffusion of H_2 in Cu (yellow); formation of Cu nanocrystallites with partially melt Cu-O-H surface layer (red sphere); segregation of the Cu/Cu-O-H core/shell nanoparticles and formation of triangle domains due to shape-complementarity. Alignment of right triangles is guided by the bi-axial texture of the CTO-Cu; and graphene nucleation on the triangles as soon as the reduction accelerates on the surface of the triangles to expose the Cu (111).

Overall, it appears that the CTO-Cu foil is a promising substrate for the growth of graphene, which could result in improved optical and electrical properties of the CVD grown graphene.

4. Experimental Section

The CTO-Cu with a thickness of 150 µm was fabricated using thermomechanical processing of base metal Cu.[38] Graphene films were grown on the copper foil in a CVD system at ~1000 °C following previously published procedures.[19] A mixture of CH_4 (3.0–35 sccm) and H_2 (0.1–2 sccm) was used for the gas precursors. The Cu substrate was put inside the fused silica furnace tube and heated to 1000 °C under H_2 flow. Growth of graphene was initiated by introduction of CH_4 after the growth temperature was reached and growth continued for 2–30 min. In order to transfer the CVD-grown graphene films onto glass or Si, poly-methyl methacrylate (PMMA) was first spin-coated on the surface of the as-grown graphene on copper. The film was then placed into iron chloride solution (0.1 g/mL) to remove the copper foil and was rinsed in DI water three times. The target substrate was then immersed into the solution and used to lift the graphene film from the liquid. The sample was placed into oven at 80 °C for one hour for drying. Finally, the PMMA was removed with acetone.

The structure and morphologies of graphene on Cu substrates were examined with scanning electron microscopy (Jeol JSM-6380 and Leo 1550 FESEM) with the electron beam accelerating voltage of 2 KeV. The electron backscatter diffraction patterns (EBSP) were used to examine recrystallization and grain orientation of Cu substrates during growth of graphene. The samples were placed in the Leo 1550 FESEM and inclined approximately 70° relative to normal incidence of the electron beam for sensitive detection of the EBSD patterns. The detector is actually a camera equipped with a phosphor screen with a digital frame grabber.

AFM images were obtained in ambient conditions using a Multimode Nanoscope E Atomic Force Microscope (Veeco Instruments, Santa Barbara CA) operating in contact mode. Veeco silicon nitride tips with a force constant of 0.12 N/m were scanned at 2 Hz with a set point of approximately 1–2 V for all images. All RMS roughness values were retrieved from flattened images with the roughness analysis feature available in the Nanoscope 5.30r3sr3 software package. Fourteen areas ranging from 9–81 μm^2 were analyzed from three separate images of each sample, and averaged for mean RMS values. For step height analysis, approximately 50 different cross sectional cuts were analyzed from several different images.

The Raman spectra were recorded using a Renishaw InVia Raman Microprobe equipped with a Helium-cadmium laser at 442 nm excitations. The laser spot is ~2 µm in diameter on the sample, and its energy density is ~1 $mW/\mu m^2$. The spectrum was taken by averaging over 10 scans.

Acknowledgements

The authors acknowledge support in part by ARO contract No. ARO-W911NF-09–1–0295 and NSF contracts Nos. NSF-DMR-0803149, 1105986 and NSF EPSCoR-0903806, and matching support from the State of Kansas through Kansas Technology Enterprise Corporation. Use of Raman instrumentation at Argonne's Center for Nanoscale Materials was supported by the USDOE, Office of Science, Office of Basic Energy Sciences. The work performed at the Argonne National Laboratory was carried out under contract DE-AC02-06CH11357 between UChicago Argonne, LLC and the USDOE. The work at Oak Ridge National laboratory was supported by the Office of Electricity Delivery and Energy Reliability, Advanced Cables and Conductor Program and Materials Sciences and Engineering Division, Office of Basic Energy Sciences, Department of Energy.
Note: This article was amended on October 21, 2011 to correct a mistake in the Experimental Section.

Received: June 9, 2011
Published online: September 13, 2011

[1] K. S. Novoselov, A. K. Geim, S. V. Morozov, D. Jiang, Y. Zhang, S. V. Dubonos, I. V. Grigorieva, A. A. Firsov, *Science* **2004**, *306*, 666.
[2] A. K. Geim, K. S. Novoselov, *Nat. Mater.* **2007**, *6*, 183.
[3] K. S. Novoselov, A. K. Geim, S. V. Morozov, D. Jiang, M. I. Katsnelson, I. V. Grigorieva, S. V. Dubonos, A. A. Firsov, *Nature* **2005**, *438*, 197.
[4] R. R. Nair, P. Blake, A. N. Grigorenko, K. S. Novoselov, T. J. Booth, T. Stauber, N. M. R. Peres, A. K. Geim, *Science* **2008**, *320*, 1308.
[5] C. Berger, Z. M. Song, X. B. Li, X. S. Wu, N. Brown, C. Naud, D. Mayou, T. B. Li, J. Hass, A. N. Marchenkov, E. H. Conrad, P. N. First, W. A. de Heer, *Science* **2006**, *312*, 1191.
[6] J. K. Wassei, R. B. Kaner, *Mater. Today* **2010**, *13*, 52.
[7] L. G. De Arco, Y. Zhang, C. W. Schlenker, K. Ryu, M. E. Thompson, C. W. Zhou, *Acs Nano* **2010**, *4*, 2865.
[8] C. Mattevi, G. Eda, S. Agnoli, S. Miller, K. A. Mkhoyan, O. Celik, D. Mostrogiovanni, G. Granozzi, E. Garfunkel, M. Chhowalla, *Adv. Funct. Mater.* **2009**, *19*, 2577.
[9] J. B. Wu, H. A. Becerril, Z. N. Bao, Z. F. Liu, Y. S. Chen, P. Peumans, *Appl. Phys. Lett.* **2008**, *92*, 263302.
[10] Z. F. Liu, Q. Liu, Y. Huang, Y. F. Ma, S. G. Yin, X. Y. Zhang, W. Sun, Y. S. Chen, *Adv. Mater.* **2008**, *20*, 3924.
[11] M. Zhou, Y. M. Zhai, S. J. Dong, *Anal. Chem.* **2009**, *81*, 5603.
[12] V. P. Verma, S. Das, I. Lahiri, W. Choi, *Appl. Phys. Lett.* **2010**, *96*, 203108.
[13] M. Dankerl, M. V. Hauf, A. Lippert, L. H. Hess, S. Birner, I. D. Sharp, A. Mahmood, P. Mallet, J. Y. Veuillen, M. Stutzmann, J. A. Garrido, *Adv. Funct. Mater.* **2010**, *20*, 3117.
[14] M. D. Stoller, S. J. Park, Y. W. Zhu, J. H. An, R. S. Ruoff, *Nano Lett* **2008**, *8*, 3498.
[15] C. Berger, Z. M. Song, T. B. Li, X. B. Li, A. Y. Ogbazghi, R. Feng, Z. T. Dai, A. N. Marchenkov, E. H. Conrad, P. N. First, W. A. de Heer, *J Phys. Chem. B* **2004**, *108*, 19912.
[16] A. Reina, X. T. Jia, J. Ho, D. Nezich, H. B. Son, V. Bulovic, M. S. Dresselhaus, J. Kong, *Nano. Lett.* **2009**, *9*, 30.
[17] X. S. Li, W. W. Cai, J. H. An, S. Kim, J. Nah, D. X. Yang, R. Piner, A. Velamakanni, I. Jung, E. Tutuc, S. K. Banerjee, L. Colombo, R. S. Ruoff, *Science* **2009**, *324*, 1312.
[18] S. Bae, H. Kim, Y. Lee, X. F. Xu, J. S. Park, Y. Zheng, J. Balakrishnan, T. Lei, H. R. Kim, Y. I. Song, Y. J. Kim, K. S. Kim, B. Ozyilmaz, J. H. Ahn, B. H. Hong, S. Iijima, *Nat. Nanotechnol.* **2010**, *5*, 574.
[19] X. S. Li, Y. W. Zhu, W. W. Cai, M. Borysiak, B. Y. Han, D. Chen, R. D. Piner, L. Colombo, R. S. Ruoff, *Nano Lett.* **2009**, *9*, 4359.
[20] X. S. Li, C. W. Magnuson, A. Venugopal, J. H. An, J. W. Suk, B. Y. Han, M. Borysiak, W. W. Cai, A. Velamakanni, Y. W. Zhu, L. F. Fu, E. M. Vogel, E. Voelkl, L. Colombo, R. S. Ruoff, *Nano Lett.* **2010**, *10*, 4328.
[21] P. Y. Huang, C. S. Ruiz-Vargas, A. M. van der Zande, W. S. Whitney, M. P. Levendorf, J. W. Kevek, S. Garg, A. S. Alden, C. J. Hustedt, Y. Zhu, J. Park, P. L. McEuen, D. A. Muller, *Nature* **2011**, *469*, 389.
[22] J. M. Wofford, S. Nie, K. F. McCarty, N. C. Bartelt, O. D. Dubon, *Nano Lett.* **2010**, *10*, 4890.
[23] Q. K. Yu, L. A. Jauregui, W. Wu, R. Colby, J. F. Tian, Z. H. Su, H. L. Cao, Z. H. Liu, D. Pandey, D. G. Wei, T. F. Chung, P. Peng, N. P. Guisinger, E. A. Stach, J. M. Bao, S. S. Pei, Y. P. Chen, *Nat. Mater.* **2011**, *10*, 443.
[24] H. Ago, I. Tanaka, C. M. Orofeo, M. Tsuji, K. Ikeda, *Small* **2010**, *6*, 1226.
[25] L. Gao, J. R. Guest, N. P. Guisinger, *Nano Lett.* **2010**, *10*, 3512.
[26] K. Mirpuri, H. Wendrock, S. Menzel, K. Wetzig, J. Szpunar, *Thin Solid Films* **2006**, *496*, 703.
[27] A. C. Ferrari, J. C. Meyer, V. Scardaci, C. Casiraghi, M. Lazzeri, F. Mauri, S. Piscanec, D. Jiang, K. S. Novoselov, S. Roth, A. K. Geim, *Phys. Rev. Lett.* **2006**, *97*.
[28] L. C. Chen, J. Y. Hwang, C. C. Kuo, K. H. Chen, *Nanotechnology* **2010**, *21*, 465705.
[29] T. G. Woodcock, J. S. Abell, J. Eickemeyer, B. Holzapfel, *J Microsc.-Oxford* **2004**, *216*, 123.
[30] J. C. Yang, B. Kolasa, J. M. Gibson, M. Yeadon, *Appl. Phys. Lett.* **1998**, *73*, 2841.
[31] C. L. H. Devlin, Y. Sato, S. Chiang. *J. Appl. Phys.* **2009**, *105*, 123534.
[32] J. A. Rodriguez, J. Y. Kim, J. C. Hanson, M. Perez, A. I. Frenkel, *Catal. Lett.* **2003**, *85*, 247.
[33] J. P. Neumann, T. Zhong, Y. A. Chang, *Bull. Alloy Phase Diagrams* **1984**, *5*, 136.
[34] Y1. Ishikawa, K. Mimura, M. Isshiki, *Materials Transactions, The Japan Institute of Metals* **1999**, *40*, 87.
[35] R. N. Barnett, U. Landman, *Phys Rev B* **1991**, *44*, 3226.
[36] T. Karabacak, J. S. DeLuca, P. I. Wang, G. A. Ten Eyck, D. Ye, G. C. Wang, T. M. Lu, *J. Appl. Phys.* **2006**, *99*.
[37] K. Moritani, M. Okada, Y. Teraoka, A. Yoshigoe, T. Kasai, *J. Phys. Chem. C* **2008**, *112*, 8662.
[38] A. Goyal, D. P. Norton, D. K. Christen, E. D. Specht, M. Paranthaman, D. M. Kroeger, J. D. Budai, Q. He, F. A. List, R. Feenstra, H. R. Kerchner, D. F. Lee, E. Hatfield, P. M. Martin, J. Mathis, C. Park, *Appl. Supercond.* **1996**, *4*, 403.